Disappearance of rotation in heavy-ion collisions

Hong Ming Xu
Cyclotron Institute, Texas A&M University, College Station, Texas 77843
(Received 8 January 1992; revised manuscript received 25 August 1992)

The azimuthal distributions of nucleons are studied for central ^{40}Ar+^{51}V collisions from $E/A = 35$ to 125 MeV based on a Boltzmann equation. We demonstrate that the contribution to azimuthal asymmetry from residue rotation decreases with incident energy and eventually vanishes at energies $E/A \geq 75$ MeV. In contrast, the contribution from the directed transverse motion remains important throughout the energy range investigated. We show that the disappearance of rotation is mainly associated with the onset of multifragmentation for which the thermal instabilities appear to play a minor role.
PACS number(s): 25.70.Pq, 21.65.+f

The azimuthal distributions of emitted particles in nucleus-nucleus collisions can carry important information concerning the reaction dynamics and the nuclear equation of state (EOS) [1,2]. At incident energies below $E/A \approx 50$ MeV, the azimuthal distributions have been investigated by using large-angle particle-particle correlations and the observed in-plane enhancements can be well explained by models incorporating the decay of a hot rotating source [3,4]. The azimuthal anisotropy decreases with incident energy [5–8] and the mechanism for such decrease is not yet understood. Recently, Garcias *et al.* [9] showed that the mass and angular momentum of a hot rotating nucleus decrease at much higher rates when the initial excitation energy and angular momentum are higher. Based on the Landau-Valsov model, they were able to explore the parameter space of energy and angular momentum and they observed all the decay channels including evaporation, fission, and multifragmentation. In their calculations, however, the entrance channel leading to the formation of the hot nuclei is not followed.

On the other hand, γ-ray circular polarization measurements [10] indicated that particles were preferably emitted to negative angles because of the attracting mean field. Moreover, the in-plane transverse momentum distributions of emitted particles were predicted [11–13], and later observed [14–17], to change sign at a certain intermediate energy, referred to as the energy of balance [14–17]. This transverse motion due to an attractive nuclear mean field at low energies or a repulsive mean field at high energies was referred to as the directed transverse motion [18].

To investigate effects of the collective rotation and the directed transverse motion and whether one can obtain new information concerning the reaction dynamics, we have performed improved Boltzmann-Uehling-Uhlenbeck (BUU) calculations for ^{40}Ar+^{51}V collisions. In our improved calculations [19–22], we have included Coulomb interactions and have used a lattice Hamiltonian method [23] to conserve the total energy. In this Brief Report, we demonstrate that both the rotational motion and the directed transverse motion play important roles at low energies in causing the in-plane enhanced emission. The contribution from rotational effects decreases with energy and eventually vanishes at energies $E/A \geq 75$ MeV. In contrast, the contribution from directed transverse motion remains important at all energies. We show that the disappearance of rotation is associated mainly with the onset of multifragmentation for which the thermal excitation energy appears to play a small role.

We simulate the Boltzmann-Uehling-Uhlenbeck equation [24]

$$\frac{\partial f_1}{\partial t} + \mathbf{v}\cdot\nabla_r f_1 - \nabla_r U\cdot\nabla_p f_1 = \frac{4}{(2\pi)^3}\int d^3k_2 d^3k_3 d\Omega \frac{d\sigma_{nn}}{d\Omega} v_{12} \times [f_3 f_4 (1-f_1)(1-f_2) - f_1 f_2 (1-f_3)(1-f_4)]\delta^3(\mathbf{k}_1+\mathbf{k}_2-\mathbf{k}_3-\mathbf{k}_4), \quad (1)$$

with the lattice Hamiltonian method of Lenk and Pandharipande [23]. In Eq. (1), $\frac{d\sigma_{nn}}{d\Omega}$ and v_{12} are the in-medium cross section and relative velocity for the colliding nucleons, and U is the total mean-field potential consisting of the Coulomb potential and a nuclear potential with isoscalar and symmetry terms [19–22]. In our calculations, we use two parameter sets [24] for the EOS which correspond to values of nuclear compressibility at $K = 200$ MeV (soft EOS) and $K = 375$ MeV (stiff EOS), respectively. For simplicity, $\sigma_{NN} = \int \frac{d\sigma_{nn}}{d\Omega} d\Omega$ is chosen to be isotropic and energy independent [24]. The mean-field and the Pauli-blocking factors in the collision integral are averaged over an ensemble of 80 parallel simulations.

To distinguish the different effects between the collective rotation and the directed transverse motion and their respective contributions in causing the azimuthal asymmetry, we follow Ref. [8] and define two simpli-

fied azimuthal parameters F_{ip} and F_{ps}. The first parameter is the fraction of particles emitted "in plane" defined as those within 45° of the reaction plane (satisfying $|\phi| \leq 45°$ or $|\phi - 180°| \leq 45°$), and the second is the fraction of particles satisfying $|\phi| \leq 90°$ or those referred to as the "projectile side" in Ref. [8]. Obviously, for azimuthally isotropic emission, both parameters would have a value of 0.5. However, when dynamics is involved, different mechanisms could cause different behavior in these two parameters.

In Fig. 1, we show both F_{ip} (solid symbols) and F_{ps} (open symbols) as a function of incident energy calculated at impact parameters $b = 2$ fm (top panel) and $b = 4$ fm (bottom), respectively. The calculations are performed at $t = 120$ fm/c, which is comparable to the freezeout times of residues [19, 20]. Nucleons are considered as emitted when their local densities are lower than 10% of the normal density. To accumulate sufficient statistics, we have included all emitted nucleons satisfying $Y \geq Y_{\rm c.m.}$; here c.m. denotes the nucleus-nucleus center of mass. The asterisks indicate F_{ip} extracted experimentally for charged particles with $Z = 2$, taken from Ref. [8]. See also Ref. [25].

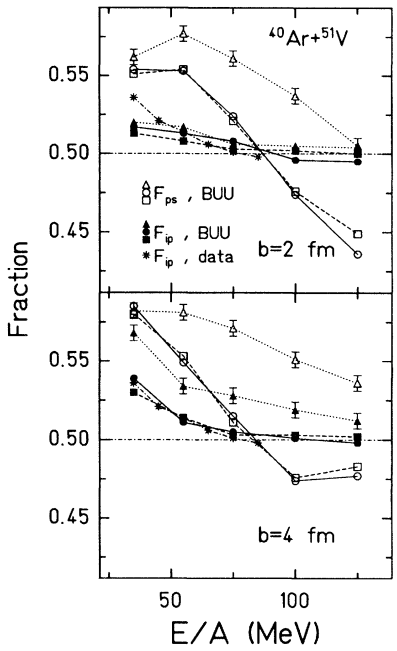

FIG. 1. Azimuthal fractions of F_{ip} (solid symbols) and F_{ps} (open symbols) are shown as a function of incident energy calculated at $b = 2$ fm (top panel) and $b = 4$ fm (bottom), respectively. The asterisks indicate experimental values of F_{ip} taken from Ref. [8]. The circles and the squares depict calculations with the stiff EOS and the soft EOS, respectively, and with σ_{NN} =41 mb. The triangles depict calculations with the stiff EOS and σ_{NN}=25 mb. Statistical uncertainties, which are similar for all calculated points, are illustrated, for the clarity of the figure, only for some selected points. The lines are used to guide the eye. Details concerning F_{ip} and F_{ps} are discussed in the text.

At low incident energies, the predicted values of both F_{ip} and F_{ps}, calculated for all input parameters, are larger than 0.5, suggesting the importance of both the collective rotation and the directed transverse motion (in this case, negative deflection due to attractive mean field) at such energies. The calculated F_{ip} has a larger value at $b = 4$ fm than that at $b = 2$ fm, reflecting larger entrance angular momenta at larger impact parameters. At higher energies, the predicted F_{ip}, at both impact parameters, decreases with incident energy, and becomes nearly isotropic at high energies $E/A \geq 75$ MeV for the calculations with σ_{NN} =41 mb, similar to the trends established by the experimental data. For the calculations with σ_{NN} =20 mb, however, F_{ip} has a value larger than 0.5 at larger impact parameters $b = 4$ fm, indicating incomplete damping of the initial reaction plane even at higher energies, if the cross section of nucleon-nucleon collision is reduced.

In contrast to rotational effects, which appear vanished at energies $E/A \geq 75$ MeV, the directed transverse motion, as revealed by F_{ps}, remains important at all energies. Because of negative deflections at low energies and positive deflections at higher energies, the predicted F_{ps} would only have a value of F_{ps}= 0.5, consistent with azimuthally isotropic emission, at a certain fixed energy, denoted as $E_{\rm iso}$. At both impact parameters, the calculated values of F_{ip} and F_{ps} are not sensitive to EOS. The value of F_{ip} is not sensitive to σ_{NN} at $b = 2$ fm, but quite sensitive to σ_{NN} at larger impact parameter $b = 4$ fm. In contrast, the value of F_{ps} is very sensitive to σ_{NN} at both impact parameters. This insensitivity to the impact parameter renders F_{ps} more useful than F_{ip} in determining σ_{NN} by comparison to experimental data. It is interesting to note here that the value of $E_{\rm iso}$ ($E_{\rm iso}/A \approx 87$ MeV, for σ_{NN}=41 mb), where F_{ps} becomes isotropic, is higher than that of the energy of balance ($E_{\rm bal}/A \approx 80$ MeV) determined by the slope of transverse momentum distributions [21]. This difference arises because of the mass asymmetry between the projectile and the target. As the mass asymmetry between projectile and target increases, the difference between $E_{\rm iso}$ and $E_{\rm bal}$ is expected to increase, and could therefore provide an additional observable for the extraction of σ_{NN} from collisions between asymmetric systems.

Compared to the experimental data, the calculations seem to exclude values of σ_{NN} below 25 mb, consistent with the predictions from the disappearance of flow [21]. The comparison must, nevertheless, be regarded as speculative, because (1) the influence of impact parameter selection on the experimental data is still not well understood; (2) uncertainties in determining the reaction plane from experimental data tend to decrease the values of F_{ip}, while exclusion of low energy particles due to detector thresholds tends to increase the value of F_{ip}; (3) clusters, not incorporated by BUU model, could show larger in-plane enhancements than nucleons [3–8]; and (4) emission due to rotating source in the final stages, not included in the present model, could provide additional enhancements [3,4], particularly at low incident energies.

What, then, causes the disappearance of rotation when

the incident energy is raised above $E/A \approx 75$ MeV? Within the prescription of a hot rotating source [3,4], such a decrease would indicate a decrease in angular momentum or an increase in temperature (thermal energy) or both. The higher the temperature, the more isotropic the emission pattern, and, therefore, the smaller the values of F_{ip}. To assess if this is indeed the case, we have decomposed the excitation energy approximately into three components, energy associated with compression or expansion, $E^*_{\rm exp}$, collective energy $E^*_{\rm coll}$, and thermal energy $E^*_{\rm the}$, respectively, using techniques similar to those outlined in Refs. [26,27]. In this decomposition, $E^*_{\rm exp}$ represents the energy change when the density distribution of the system is changed away from that of a ground state nucleus (e.g., the creation of surfaces due to multifragmentation). As shown in Fig. 2, for both the soft EOS (top panel) and the stiff EOS (bottom), the total excitation energy (squares) of residues calculated at freezeout [19, 20] increases with incident energy. In contrast, at incident energies $E/A \geq 65$ MeV, the thermal excitation energy $E^*_{\rm the}$ (circles) decreases with energy. At the same time, the energy associated with expansion, $E^*_{\rm exp}$ (difference between squares and triangles), increases rapidly. The decrease in the thermal excitation energy and the increase in the expansion energy reflect the onset of multifragmentation observed in this system within our code [22]. Thus it is the onset of multifragmentation, for which the thermal excitation energy decreases rather than increases, that plays the major role for the disappearance of flow at high energies. The rapid increase in $E^*_{\rm exp}$ occurs at slightly higher incident energy for calculations with the stiff EOS, because stiffer EOS has larger surface tension strength, so that its tendency for nucleus to break up is less (corresponding to a higher energy threshold for multifragmentation).

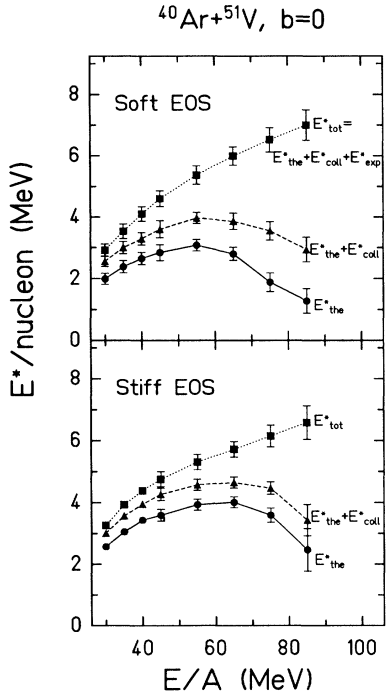

FIG. 2. Decomposition of total excitation energy (squares) into thermal energy (circles), collective energy (difference between triangles and circles), and energy associated with expansion (difference between squares and triangles) calculated for both the soft EOS (top panel) and the stiff EOS (bottom). The error bars include both statistical uncertainties as well as uncertainties associated with ground state stability. The details are discussed elsewhere in Refs. [20,22].

To examine how effects of residue rotations depend on the incident energy, we display in Fig. 3 the angular momenta [19] of bound residues [$\rho(\mathbf{r}) \geq 10\%\rho_0$] as a function of time for ^{40}Ar+^{51}V collisions at $E/A = 35$ MeV (circles), 75 MeV (squares), and 125 MeV (triangles), respectively. The numerical accuracies for angular momentum conservation are demonstrated by the open symbols which depict the total entrance channel angular momenta in the center of mass. For calculations at all three energies, the angular momenta left in the residues exhibit two distinct stages, a rather steep decrease at a early stage ($t \leq 120$ fm/c) and a slow decrease afterwards. This result is not a surprise since one expects the earlier nonequilibrium stage should have a higher emission rate than that in the later evaporation stage. The interesting point here is that the rate of decrease in the angular momentum is much larger at higher energies (for the cases we calculated, the drops in angular momenta at higher energies $E/A = 75$ and 125 MeV are so large that the angular momenta left in residues are even smaller than that at $E/A = 35$ MeV after a certain elapse of time, $t \approx 60$–70 fm/c), a result also predicted by the Landau-Valsov calculations [9] where hot rotating sources are initially provided without following the entrance channel that leads to their formation. Because the residue has not made a full cycle of rotation on the time scale which we follow, the contributions to azimuthal asym-

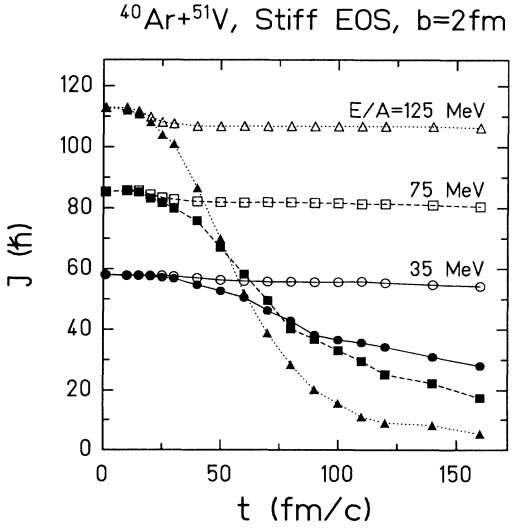

FIG. 3. Angular momenta of residues (solid symbols) as a function of time calculated at $E/A = 35$ MeV (circles), 75 MeV (squares), and 125 MeV (triangles). The open symbols show the corresponding total angular momenta in the nucleus-nucleus center of mass. The lines are used to guide the eye.

metry from later residue rotations would be smaller at higher energies, simply because they have smaller angular momenta. At low energy $E/A = 35$ MeV, emission from residue rotation [3,4] could provide additional in-plane enhancement to F_{ip}, because the residue still has a non-negligible angular momentum $J \approx 35\hbar$ at the time when F_{ip} is evaluated.

In conclusion, with an improved BUU model, we have investigated the dynamical origins of the azimuthal asymmetry in central ^{40}Ar+^{51}V collisions. We show that the contributions to azimuthal asymmetry from collective rotating residues decrease with incident energy and eventually vanish at energies $E/A \geq 75$ MeV. In contrast, the directed transverse motion due to the nuclear mean field remains important at all energies. We demonstrate that the disappearance of rotations at higher incident energies is associated mainly with the onset of multifragmentation for which the thermal excitation energy appears to decrease with incident energy. We propose that measurements of $E_{\rm iso}$, at which the azimuthal distributions are consistent with isotropic emission, as revealed by F_{ps}, could provide an additional tool to pin down accurately the in-medium nucleon-nucleon cross section from collisions between asymmetric systems.

The author would like to acknowledge C.A. Gagliardi, C.M. Ko, J.B. Natowitz, R.P. Schmitt, R.E. Tribble, and D.H. Youngblood for valuable advice and support. Stimulating discussions with G.F. Bertsch, P. Danielewicz, C.K. Gelbke, and W.G. Lynch at early stages of this work are warmly welcome. This work was supported in part by the Department of Energy under Grant No. DE-FG05-86ER40256 and by the Robert A. Welch Foundation.

[1] G. M. Welke, M. Prakash, T. T. S. Kuo, S. Das Gupta, and C. Gale, Phys. Rev. C **38**, 2101 (1988).
[2] C. Hartnack, H. Stöcker, and W. Greiner, in *Proceedings of the NATO Summer School on The Nuclear Equation of State*, Peñiscola, Spain, 1989, Vol. 215A of *NATO Advanced Study Institute Series B: Physics*, edited by W. Greiner and H. Stöcker (Plenum, New York, 1989), p. 239.
[3] M. B. Tsang *et al.*, Phys. Rev. Lett. **52**, 1967 (1984); Phys. Lett. **148B**, 265 (1984); Phys. Rev. C **42**, R15 (1990); **44**, 2065 (1991).
[4] C. B. Chidwood *et al.*, Phys. Rev. C **34**, 858 (1986).
[5] H. J. Rabe *et al.*, Phys. Lett. B **196**, 439 (1987).
[6] P. Kristiansson *et al.*, Phys. Lett. **155B**, 31 (1985).
[7] D. Ardouin *et al.*, Nucl. Phys. **A447**, 585c (1985).
[8] W. K. Wilson *et al.*, Phys. Rev. C **41**, R1881 (1990).
[9] F. Garcias, V. De La Mota, B. Remaud, G. Royer, and F. Sébille, Phys. Lett. B **255**, 311 (1991).
[10] M. B. Tsang *et al.*, Phys. Rev. Lett. **60**, 1479 (1988); **57**, 559 (1986).
[11] J.J. Molitoris and H. Stöcker, Phys. Lett. **162B**, 47 (1985).
[12] G. F. Bertsch, W. G. Lynch, and M. B. Tsang, Phys. Lett. B **189**, 384 (1987).
[13] A. Bonasera and L. P. Csernai, Phys. Rev. Lett. **59**, 630 (1987).
[14] D. Krofcheck *et al.*, Phys. Rev. Lett. **63**, 2028 (1989).
[15] C. A. Ogilvie *et al.*, Phys. Rev. C **42**, R10 (1990).
[16] D. Krofcheck *et al.*, Phys. Rev. C **43**, 350 (1991).
[17] J. P. Sullivan *et al.*, Phys. Lett. B **249**, 8 (1990).
[18] C. A. Ogilvie *et al.*, Phys. Rev. C **40**, 2592 (1989); Phys. Lett. B **231**, 35 (1989).
[19] H. M. Xu, W. G. Lynch, P. Danielewicz, and G. F. Bertsch, Phys. Rev. Lett. **65**, 843 (1990); Phys. Lett. B **261**, 240 (1991).
[20] H. M. Xu, P. Danielewicz, and W. G. Lynch, Phys. Lett. B (in press).
[21] H. M. Xu, Phys. Rev. Lett. **67**, 2769 (1991); Phys. Rev. C **46**, R389 (1992).
[22] H. M. Xu, Phys. Rev. C **46**, R2144 (1992).
[23] R.J. Lenk and V.R. Pandharipande, Phys. Rev. C **39**, 2242 (1989).
[24] G. F. Bertsch and S. Das Gupta, Phys. Rep. **160**, 189 (1988), and references therein.
[25] In Ref. [8], data for $Z = 1$ were also extracted at target rapidities. Because of large detector thresholds for these low rapidity particles, the measured spectra exhibited large distortions, and were therefore not included in Fig. 2.
[26] B. Remaud, C. Grégoire, F. Sébille, and P. Schuck, Nucl. Phys. **A488**, 423c (1988).
[27] E. Suraud *et al.*, Phys. Lett. B **229**, 359 (1989).